

Study of Intramolecular Competition between Carboxylate and Phosphonate for Pt^{II} with the Aid of a Novel Tridentate Carboxylato-Thioether-Phosphonato Ligand

Matthieu Hamel,^[b] Silvia Rizzato,^[c] Matthieu Lecinq,^[b] Aboubacary Sène,^[d] Michel Vazeux,^[b] Mihaela Gulea,^[b] Alberto Albinati,^[c] and Jiří Kozelka*^[a]

Abstract: The tridentate dianionic ligand 2-[2'-(hydroxyisopropoxyphosphoryl)phenylsulfanyl]benzoate (L^{2-}) reacts with *cis*-[Pt(NH₃)₂(H₂O)₂]²⁺ to form an S,O-chelate in which the O-coordinated group is either carboxylate or phosphonate, depending on the degree of protonation of the complex. Carboxylate appears to be the stronger ligand, and the stoichiometric reaction between *cis*-[Pt(NH₃)₂(H₂O)₂]²⁺ and L^{2-} yields the neutral species [Pt(L)(NH₃)₂], with L bound by sulfanyl and carboxylate groups, both in solution

and in the solid state. Upon protonation of [Pt(L)(NH₃)₂], the stronger basicity of the carboxylate causes the Pt coordination to switch from carboxylate to phosphonate, and the uncoordinated carboxylate group becomes protonated. In methanolic solution, the first-order kinetics of this rearrange-

ment could be observed by ³¹P NMR spectroscopy. Both complexes—the carboxylate-bound neutral complex [Pt(L)(NH₃)₂]·H₂O (triclinic, $P\bar{1}$ (no. 2), $a=9.529(6)$, $b=9.766(6)$, $c=12.299(7)$ Å, $\alpha=106.91(2)$, $\beta=101.71(2)$, $\gamma=102.05(2)^\circ$, $Z=2$) and the perchlorate salt of the phosphonate-bound complex [Pt(LH)(NH₃)₂]ClO₄·H₂O (monoclinic, $P2_1/c$ (no. 14), $a=12.095(2)$, $b=14.046(2)$, $c=14.448(2)$ Å, $\beta=95.55(2)^\circ$, $Z=4$)—were characterized by X-ray crystallography.

Keywords: carboxylate ligands • intramolecular ligand competition • phosphonate ligands • platinum • S ligands

Introduction

cis-Diamminedichloroplatinum(II) (*cis*-[PtCl₂(NH₃)₂], “cis-platin”) is a widely used antitumor drug whose activity is believed to be related to its DNA-binding capacity.^[1,2] Its medical use is restricted by the relatively narrow spectrum of tumors against which it is highly active, and also in certain patients by the development of resistance.^[3,4] One possible strategy in the development of more potent drugs is based on functionalization of the platinum complex with groups that have affinity for specific receptors,^[5] organs,^[6] or biomolecules,^[7] thus allowing for targeted delivery. Following this line, Keppler et al. have designed aminobisphosphonate derivatives of platinum(II) diamine complexes that possess osteotropic properties, due to the affinity of the phosphonate group for Ca²⁺.^[8,9] Recently, oxidized single-wall carbon nanohorns have been shown to have potential as a drug delivery system for cisplatin,^[10] which was noncovalently entrapped in these carbon nanoparticles. Some related nanoparticles, carbon nanotubes (CNTs), are emerging functionalizable nanovectors for drug delivery, allowing a drug

[a] Dr. J. Kozelka
Laboratoire de Chimie et Biochimie Pharmacologiques et Toxicologiques
Université René Descartes, UMR CNRS 8601
45, rue des Saints-Pères, 75270 Paris Cedex 06 (France)
Fax: (+33) 142868387
E-mail: jiri.kozelka@univ-paris5.fr

[b] Dr. M. Hamel, M. Lecinq, Dr. M. Vazeux, Dr. M. Gulea
Laboratoire de Chimie Moléculaire et Thio-organique
UMR CNRS 6507
Université de Caen, ENSICAEN
6, Bld. Maréchal Juin, 14000 Caen (France)

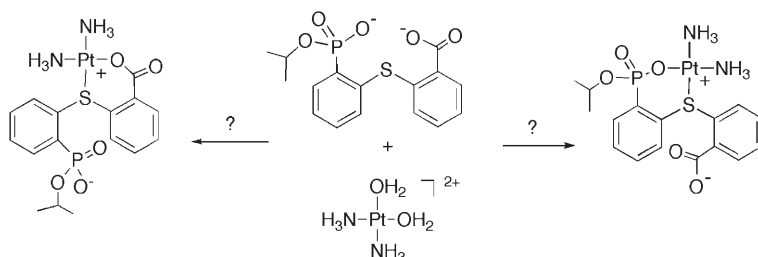
[c] Dr. S. Rizzato, Prof. A. Albinati
Dipartimento di Chimica Strutturale e Stereochimica Inorganica
Università di Milano
via G. Venezian 21, 20133 Milano (Italy)

[d] Dr. A. Sène
Laboratoire de chimie des produits naturels
Université Cheikh Anta Diop
Dakar-Fann (Sénégal)

Supporting information for this article is available on the WWW under <http://www.chemeurj.org/> or from the author.

to be linked to the nanotube by means of a weak covalent bond.^[11]

Because of its potential for application as a Pt^{II}-chelating ligand capable of attachment to a functionalized carrier molecule, we have synthesized the trifunctional ligand 2-[2'-(hydroxyisopropoxyphosphoryl)phenylsulfanyl]benzoic acid (**LH**₂), the deprotonated form of which (**L**²⁻) contains one carboxylate, one phosphonate monoester, and one thioether group (Scheme 1). The potassium salt of **L**²⁻ reacted with the diaqua form of cisplatin (*cis*-[Pt(NH₃)₂(H₂O)₂]²⁺) to yield the complex [Pt(**L**)(NH₃)₂] (**1a**), protonation of which with HClO₄ (1 equiv) afforded the ionic compound [Pt(**LH**)(NH₃)₂]⁺ClO₄⁻ (**1b**). Two chelation modes of a *cis*-[Pt(NH₃)₂]²⁺ moiety by **L**²⁻ are conceivable:



a six-membered metallacycle involving the thioether group and the carboxylate group, and a six-membered metallacycle involving the thioether group and the phosphonate group. Which acido group is coordinated in **1a** and **1b** was not clear a priori, as the relative capacities of a phenylcarboxylate versus a phenylphosphonate monoester to bind to Pt^{II} were unknown. Neither was it clear which of the two acido groups would be the stronger base. In a related system with *N*-(phosphonomethyl)glycine (impaH₃), in which the secondary amine group and either acido group (carboxylate or phosphonate) can form a five-membered ring with Pt^{II}, Appleton et al. found that the fully deprotonated complex [Pt(impa)(NH₃)₂]⁻ was coordinated by the phosphonate group whereas the doubly protonated complex [Pt(impaH₂)(NH₃)₂]⁺ was coordinated by the carboxylate group.^[12] We were able to obtain monocystals of each complex **1a** and **1b** and to demonstrate by means of X-ray diffraction analysis that in our case the situation is reversed: the fully deprotonated form **1a** features carboxylate coordination to platinum, whereas the protonated form **1b** has the phosphonate monoester coordinated. Moreover, we were able to follow, by ³¹P NMR, the rearrangement from the carboxylate-bound **1a** to the phosphonate-bound **1b** upon protonation in meth-

anol. The results are discussed in terms of coordinating affinity, relative acidity, and steric strain.

Results

Synthesis of 2-[2'-(hydroxyisopropoxyphosphoryl)phenylsulfanyl]benzoic acid (LH**₂):** This trifunctional ligand was synthesized as shown in Scheme 1, by Cu₂O-catalyzed coupling of diisopropyl 2-sulfanylphenylphosphonate^[13,14] with 2-iodobenzoic acid, as reported by Ferretti and Adams,^[15] and hydrolysis of the diphenyl sulfide bearing the diisopropylphosphonate group by treatment with sodium azide under the conditions described by Holy.^[16] The overall yield of the two steps was 62%.

Titration of **LH₂ in methanol, monitored by ³¹P NMR spectroscopy:** **LH**₂ (0.05 mmol) was dissolved in CD₃OD (0.45 mL) and titrated in an NMR tube with portions of KOH (1/3 equiv, added as a 1.67 M solution in CD₃OD). The ³¹P chemical shift is plotted against the number of equivalents of KOH added in

Figure 1. It can be seen that δ_P decreases monotonically (shifts upfield) during the addition of the first equivalent of KOH, while during the addition of the second equivalent, δ_P changes only slightly and passes through a minimum. This

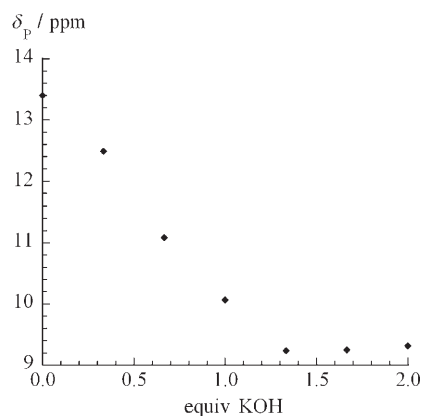


Figure 1. ³¹P chemical shift of a sample of **LH**₂ (0.05 mmol) dissolved in CD₃OD (0.45 mL) and titrated with portions of KOH (1/3 equiv, added as 1.67 M solution in CD₃OD), as a function of the number of added KOH equivalents. *T* = 297 K.

Scheme 1. Pathway for the synthesis of **LH**₂.

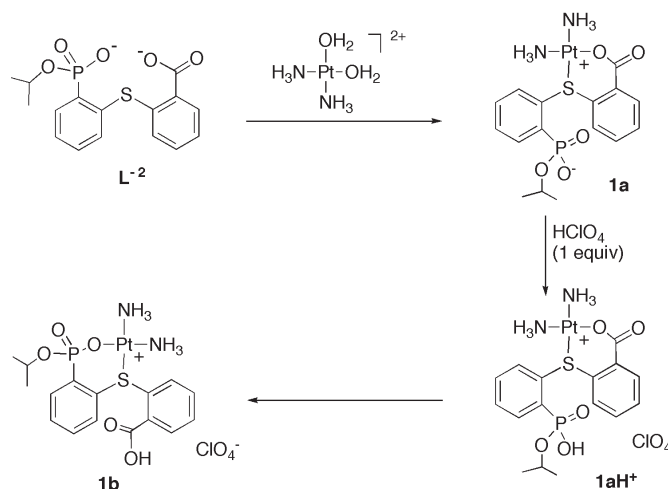
behavior indicates that the phosphonate group is deprotonated first. Deprotonation of a phosphonate is commonly accompanied by an upfield shift of the δ_p signal.^[17] The δ_p values of **LH**₂ and **L**²⁻ in methanol, according to Figure 1, are 13.4 and 9.3 ppm, respectively. The phosphorus atom of the monoprotonated form (**LH**⁻) apparently resonates slightly upfield from that of **L**²⁻, at about $\delta_p=9.1$ ppm. This slight upfield shift is the result both of changes in electronic population and of conformational changes accompanying the deprotonation of the carboxylate group. At 1 equiv KOH added, **LH**⁻ is in equilibrium with both **LH**₂ and **L**²⁻, and the δ_p value of 10.06 ppm reflects this equilibrium. It is noteworthy that the ³¹P signal of **LH**₂ was relatively broad and became monotonically thinner upon titration to **LH**⁻ and **L**²⁻, presumably reflecting the exchange of polar protons or exchange between different hydrogen-bonded conformations. When small portions of HClO₄ in CD₃OD were added to the tube containing **L**²⁻ in order to restore **LH**⁻ and **LH**₂ successively, the same curve as shown in Figure 1 (within error due to concentration measurements) was observed; however, now and in a following titration cycle (with KOH again), the signal of **LH**⁻ was broader than that of either **LH**₂ and **L**²⁻. We believe that this difference from the first titration step was due to traces of H₂O present in the KOH and HClO₄ solutions. Water can mediate proton exchange and participate in the conformational equilibria involving switches in hydrogen bonding. Cooling of the sample containing 1 equiv KOH to -50 °C in the third titration cycle produced a single, narrow ³¹P signal.

Reaction between **L²⁻ and *cis*-[Pt(NH₃)₂(H₂O)₂]²⁺:** The ligand **LH**₂, doubly deprotonated with KOH, reacted readily with aqueous *cis*-[Pt(NH₃)₂(H₂O)₂]²⁺ to give analytically pure [Pt{**L**-S,(OC)}(NH₃)₂]₂·H₂O (**1a**) in good yield. The coordination through the thioether and carboxylate groups was established by X-ray crystallography (vide infra). Complex **1a** is insoluble in water but sufficiently soluble in MeOH and DMF to enable recording of ¹⁹⁵Pt NMR spectra, which consist of single peaks at $\delta=-2585$ and -2581 ppm, respectively, consistently with a PtN₂OS coordination sphere.^[18]

Acid-induced isomerization of Pt(S,OC)-chelate (1a**) to Pt(S,OP)-chelate (**1b**):** The carboxylate group of **L**²⁻ was shown above to be a better ligand for Pt^{II} than the phosphonate monoester group; the titration of **LH**₂, on the other hand, indicated that carboxylate is also the better base. The intriguing question then arose of whether protonation of **1a** might be able to induce a coordination switch from carboxylate to phosphonate, with concomitant proton transfer to the carboxylate group. Treatment of **1a** with perchloric acid was therefore followed by ³¹P NMR spectroscopy. Addition of HClO₄ (1 equiv) to the methanolic solution of **1a** immediately generated [Pt{**LH**-S,(OC)}(NH₃)₂]₂ClO₄ (**1aH**⁺) with protonation of the uncoordinated phosphonate moiety, and this protonation was reflected in a downfield shift of the ³¹P resonance from 6.36 ppm in **1a** to 9.88 ppm in **1aH**⁺. Phosphonate ³¹P signals typically show a downfield shift upon protonation (vide infra).^[17] When the system was allowed to

stand at room temperature a new ³¹P peak at 11.04 ppm appeared and grew at the expense of that at 9.88 ppm, following first-order kinetics ($k=(7.0\pm 0.3)\times 10^{-5}$ s⁻¹ at 23 °C). After 48 h, the ³¹P NMR spectrum consisted almost solely of the peak at 11.04 ppm, together with a small ($\approx 10\%$) peak corresponding to the protonated ligand **LH**₂ at 13.4 ppm. It is possible that the perchloric acid had been added in a slight excess and that a small fraction of **L**²⁻ had been doubly protonated to **LH**₂ and detached from platinum. Addition of THF to this methanolic solution induced crystallization of an isomer of **1aH**⁺, [Pt{**LH**-S,(OP)}(NH₃)₂]₂ClO₄·H₂O (**1b**), in which the phosphonate is coordinated and the carboxylate protonated. Thus, **1aH**⁺ does indeed rearrange in methanol, with proton transfer from the phosphonate site to carboxylate and a concomitant switch from carboxylate to phosphonate coordination. The ¹⁹⁵Pt chemical shift of **1b** in DMF is -2475 ppm, suggesting that the coordination sphere in this species closely resembles that in **1a**. Unambiguous confirmation of the coordination through the thioether and phosphonate groups in **1b** was provided by X-ray crystallography (vide infra).

The rearrangement from **1aH**⁺ to **1b** (Scheme 2) implies changes in electron density on several carbon atoms, and one referee suggested that the rearrangement might also be followable by ¹³C NMR. The poor solubility of **1b** in methanol (6 mg mL⁻¹ at room temperature), however, precluded the acquisition of well resolved ¹³C NMR spectra.



Scheme 2. Formation of **1a** and **1b** from **L**²⁻.

Crystal structures of [Pt{L**-S,(OC)}(NH₃)₂]₂·H₂O (**1a**) and [Pt{**LH**-S,(OP)}(NH₃)₂]₂ClO₄·H₂O (**1b**):** The crystal structures of **1a** and **1b** were determined by single-crystal X-ray diffractometry in order to investigate the binding mode of the **L**²⁻ ligand as a function of its degree of protonation. The crystal structure of the diprotonated ligand **LH**₂ was also solved for comparison, and important bond distances and angles for all three compounds are listed in Table 1. The molecular structures, together with the numbering schemes for the main atoms, are illustrated in Figure 2.

Table 1. Selected interatomic distances [Å] and angles [°] for compounds **1a**, **1b**, and **LH₂**.

Compound 1a			
Pt–O1a	2.010(2)	O1a–Pt–N2	85.5(1)
Pt–N1	2.026(3)	N1–Pt–N2	89.1(1)
Pt–N2	2.053(3)	O1a–Pt–S	93.78(7)
Pt–S	2.2534(9)	N1–Pt–S	91.69(9)
P–O2	1.493(3)	O2–P–O3	115.8(2)
P–O3	1.502(3)	O2–P–O1	110.1(2)
P–O1	1.593(3)	O3–P–O1	111.0(2)
P–C1	1.818(4)	O2–P–C1	109.0(2)
S–C6	1.817(3)	O3–P–C1	109.8(2)
S–C7	1.790(3)	O1–P–C1	100.0(2)
C7–C12	1.392(5)	C7–S–C6	102.5(2)
C12–C13	1.516(5)	C7–S–Pt	104.1(1)
C13–O2a	1.236(4)	C6–S–Pt	111.4(1)
C13–O1a	1.279(4)	C12–C7–S	124.9(3)
		C7–C12–C13	126.4(3)
		O2a–C13–O1a	121.0(3)
		O2a–C13–C12	117.2(3)
		O1a–C13–C12	121.8(3)
		C13–O1a–Pt	130.9(2)
		C2I–O1–P	124.9(2)
		C5–C6–S	120.9(3)
		C1–C6–S	117.6(3)
Compound 1b			
Pt–O3	2.026(3)	O3–Pt–N2	88.4(2)
Pt–N1	2.034(4)	N1–Pt–N2	89.9(2)
Pt–N2	2.049(4)	O3–Pt–S	89.4(1)
Pt–S	2.270(1)	N1–Pt–S	92.2(1)
P–O2	1.482(4)	O2–P–O3	117.8(2)
P–O3	1.528(4)	O2–P–O1	108.4(2)
P–O1	1.574(4)	O3–P–O1	107.0(2)
P–C1	1.810(5)	O2–P–C1	108.7(2)
S–C6	1.796(5)	O3–P–C1	109.4(2)
S–C7	1.816(5)	O1–P–C1	104.7(2)
C1–C6	1.405(7)	C2I–O1–P	125.1(3)
C12–C13	1.49(1)	C6–S–Pt	106.9(2)
C13–O1a	1.180(9)	C7–S–Pt	104.9(2)
C13–O2a	1.325(7)	C6–S–C7	102.3(2)
		P–O3–Pt	111.8(2)
		C6–C1–P	127.0(4)
		C1–C6–S	125.0(4)
		C5–C6–S	113.3(4)
		C12–C7–S	120.2(5)
		C7–C12–C13	121.2(6)
		O1a–C13–O2a	121.3(7)
		O1a–C13–C12	124.5(6)
		O2a–C13–C12	114.2(7)
Compound LH₂			
P–O2	1.481(7)	O2–P–O3	110.9(5)
P–O3	1.539(7)	O2–P–O1	113.9(5)
P–O1	1.54(1)	O3–P–O1	109.2(6)
P–C1	1.87(2)	O2–P–C1	112.1(8)
C6–S	1.75(2)	O3–P–C1	108.3(8)
S–C7	1.77(1)	O1–P–C1	102.0(7)
C12–C13	1.61(2)	C1–C6–S	129(2)
C13–O2a	1.18(3)	C5–C6–S	117(2)
C13–O1a	1.26(2)	C6–S–C7	103.5(6)
		C12–C7–S	120.3(8)
		C8–C7–S	119.9(9)
		C7–C12–C13	126(1)
		C11–C12–C13	113(2)
		O2a–C13–O1a	130(2)
		O2a–C13–C12	116(2)
		O1a–C13–C12	114(2)

The structure of **1a** is based on packing of [Pt(L)(NH₃)₂] and water molecules interconnected through a network of hydrogen bonds (see Figure S1 in the Supporting Information). The Pt^{II} ion has a slightly distorted square planar coordination and the thioether and carboxylate groups of L²⁻ chelate the Pt atom, forming a six-membered ring. The deviations from the best plane defined by the Pt, O1a, S, N1, and N2 atoms are within 0.016(1) and 0.054(1) Å. In the electroneutral complex **1a**, the coordination of the doubly deprotonated ligand L²⁻ through the sulfide and carboxylate functionalities results in a significant difference between the two C–O bond lengths: 1.279(4) and 1.236(4) Å for the coordinated and free carboxylate oxygens, respectively. Conversely, the P–O2 and P–O3 distances (1.493(3) and 1.502(3) Å, respectively) are very similar and intermediate between the average values reported for a single and a double P–O bond, suggesting a significant delocalization of the negative charge.^[19]

In compound **1b** the LH⁻ ligand binds to the platinum(II) center through the sulfur atom and an oxygen atom of the anionic phosphonate group, again forming a six-membered ring. The Pt^{II} ion has an almost perfect square planar environment with a maximum deviation from the best plane defined by Pt, O3, S, N1, and N2 of 0.017(2) Å. The two C–O bond lengths in the now protonated carboxylic group (C13–O1a 1.180(9), C13–O2a 1.325(7) Å) compare well with the average values reported for a single and a double C–O bond, respectively, confirming the presence of distinct carbonyl and hydroxy units. In this complex the P–O2 bond is significantly shorter than P–O3 (ca. 0.05 Å), arising from the coordination of O3 to the metal center. Finally, in both **1a** and **1b** the Pt–N bond *trans* to the sulfur atom (2.053(3) Å and 2.049(4) Å, respectively) is slightly longer than that *trans* to the oxygen atom (2.026(3) and 2.034(4) Å, respectively), a manifestation of the larger *trans* influence of the sulfur atom.^[20] The crystal of **1b** also contains a ClO₄⁻ anion in a 1:1 ratio with the cationic complex and a water molecule participating, as in **1a**, in a hydrogen bonding network (see Figure S2 in the Supporting Information).

Figure 3 shows the structures of **1a** and **1b** in two different orientations that highlight the different conformations of the tridentate ligand. In the top view the structures were aligned according to the phenyl ring bearing the carboxylate functional group, while in the bottom view the structures share the orientation of the phosphonate-substituted phenyl ring. The two views make it clear that the mutual orientations of the phenyl rings in **1a** and **1b** are very different. The conformation of LH⁻ chelating platinum through the thioether and phosphonate groups in **1b** is relatively similar to that found in the free diacid LH₂. Apparently, only a small conformational rearrangement of the ligand is necessary to chelate platinum in this way. On the other hand, a relatively large conformational change accompanies the chelation through the thioether and carboxylate groups in **1a**. Probably the most energetically costly part of this conformational adaptation of the ligand involves the carboxylate group, which is rotated away from the phenyl group by

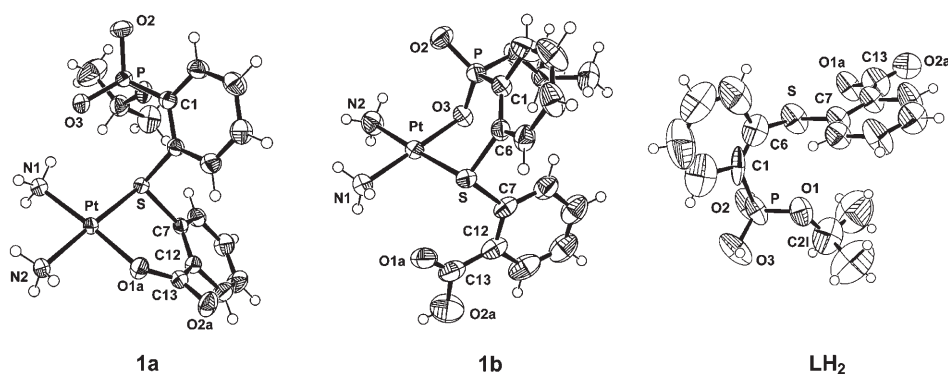


Figure 2. ORTEP views (50% probability ellipsoids) of crystal structures of **1a**, **1b**, and **LH₂** showing the coordination of platinum and displaying the atom numbering. Counterions and crystal water molecules are omitted.

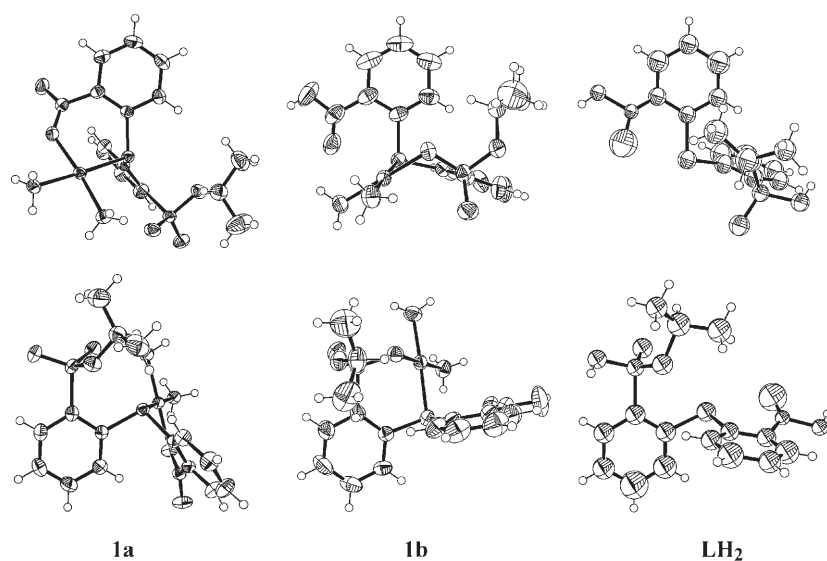


Figure 3. ORTEP views of **1a**, **1b**, and **LH₂**, aligned so that the carboxyphenyl groups (top) or the phosphonophenyl groups (bottom) have the same orientations.

29.04(7)° obviously in order to accommodate platinum coordination (see Figure 2).

Although ligand **LH₂** is achiral, coordination of the thioether group to platinum fixes the chirality at the sulfur atom. Complex **1a** thus exists as a pair of enantiomers, and the centrosymmetric unit cell (space group $P\bar{1}$) contains one molecule of each enantiomer (only the *R* enantiomer is shown in Figures 2 and 3). In complex **1b**, coordination of the phosphonate group to platinum has created a second chiral center on the phosphorus atom. Only the (*R,S/S,R*) diastereomer was formed upon crystallization, as can be seen in Figures 2 and 3 (the molecule shown has the *R,S* configuration at the P and S centers). The second pair of enantiomers—*R,R* and *S,S*—is apparently energetically less favored. This is probably the case in solution as well, since we observe only one ³¹P and one ¹⁹⁵Pt NMR signal, and only one set of ¹H NMR signals. Strictly speaking, however, we

have no proof that the pair of enantiomers present in solution is the same as that observed in the crystals, since no structural study in solution was undertaken.

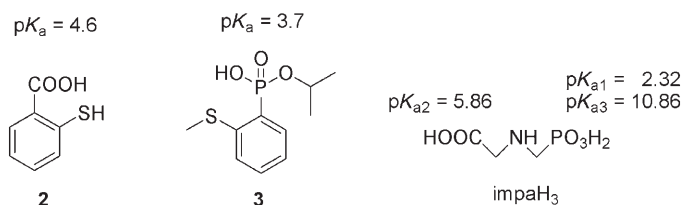
Discussion

Carboxylate and phosphonate groups are weak ligands for Pt^{II}. Their incorporation into bi- or polydentate ligands makes their coordination to Pt^{II} less labile because of the chelate effect; however, substitution by nucleic bases remains feasible. Thus, the antitumor drug carboplatin—diammine-cyclobutylidicarboxylatoplatinum(II)^[1]—forms base–base crosslinks with DNA similarly to cisplatin, but reacts about 100 times more slowly.^[21] A number of platinum complexes bearing multidentate ligands with phosphonate groups have been designed by Keppler et al. as potential drugs against bone malignancies and showed cytotoxic properties against various cell lines; it can be supposed that these complexes also react with DNA upon decoordination of the phosphonate group.^[8,9,22] Recently, Natile et al. have reported the synthesis of Pt^{II} complexes with diethyl[(methylsulfinyl)-methyl]phosphonate, in consideration of their potential as anticancer drugs.^[23]

The ligand **L²⁻**, the synthesis of which is reported here, contains a carboxylate and an isopropylphosphonate group as substituents of phenyl rings in a symmetrical relationship with respect to a sulfide functionality bridging both phenyls. When **L²⁻** reacts with Pt^{II}, the soft S atom would be expected to coordinate the metal first.^[24] Both the carboxylate and the phosphonate groups then have the potential to react with platinum, to form a six-membered chelate ring. To study this intramolecular competition was the central aim of this work. The crystal structures of **1a** and **1b** show that, when the ligand **L** is fully deprotonated (such as in **1a**), the coordinating acido group is carboxylate. On the other hand, when the ligand is monoprotonated (such as in **1b**), the coordinating group is phosphonate. The structures suggest that there is significantly larger strain in the Pt-S-C-C-C-O ring

of **1a** than in the Pt-S-C-C-P-O ring of **1b**. First, the deviations of the endocyclic bond angles from their ideal values are larger in **1a** than in **1b**. Second, the coordination of the carboxylate in **1a** requires the C13-O1a-O2a plane of the carboxylate group to rotate by 29° out of the phenyl ring plane, impeding optimal π delocalization between the carbonyl bond and the phenyl ring. In spite of the larger strain in the six-membered ring involving platinum-bound carboxylate, this functional group coordinates platinum in **1a**. This observation indicates that carboxylate is a better ligand for Pt^{II} than phosphonate, at least in the given context.

Why then, does the coordination switch from carboxylate to phosphonate upon protonation? In the complex **1a**, in which the ligand **L**²⁻ is fully deprotonated, the larger intrinsic affinity of carboxylate for platinum apparently outweighs the larger strain in the six-membered Pt-S-C-C-C-O ring in relation to the Pt-S-C-C-P-O ring. In **1b**, in which **L**²⁻ has been protonated to form **LH**⁻, a third factor—the relative basicity of the acido groups—enters into play. The coordination switch from carboxylate to phosphonate upon protonation suggests that the phenylcarboxylate entity is a stronger base than isopropyl phenylphosphonate. This had already been indicated by the titration of **LH**₂ with KOH in methanol (vide supra). The p*K*_a values of the carboxylate and phosphonate ester groups of **LH**₂ could not be determined because of the poor solubility of **LH**₂ in water; however, approximate p*K*_a values could be obtained from titrations of two model compounds containing carboxylate and phosphonate functionalities, respectively, in environments similar to those in **LH**₂. Thus, thiosalicylic acid (**2**) and isopropyl 2-



(methylsulfanyl)phenylphosphonic acid monoester (**3**) were titrated in methanol/water 10:90 v/v, yielding p*K*_a values of 4.6 and 3.7, respectively (27 ± 2 °C, experiments in duplicate, estimated p*K*_a error ± 0.1). These titrations confirm that phenylcarboxylate containing an *ortho*-sulfanyl group is a stronger base than isopropyl phenylphosphonate monoester. We can therefore conclude that when **LH**⁻ coordinates *cis*-[Pt(NH₃)₂]²⁺ in **1b**, the stronger basicity of the carboxylate group and the relatively strainless coordination of phosphonate outweigh the intrinsically stronger affinity of carboxylate for platinum, resulting in phosphonate coordination and protonation of carboxylate.

Phosphonate versus carboxylate coordination in complexes [Pt(NH₃)₂(impaH_n)]⁽ⁿ⁻¹⁾⁺ (impaH₃ = *N*-(phosphonomethyl)glycine).^[12] It may appear intriguing that a coordination switch opposite to that between **1a** and **1b** has been observed in the related system of *cis*-[Pt(NH₃)₂(H₂O)₂]²⁺ and

N-(phosphonomethyl)glycine (impaH₃): whereas the fully deprotonated species—[Pt(NH₃)₂(impa)]⁻—is coordinated by the phosphonate group, the diprotonated species—[Pt(NH₃)₂(impaH₂)]⁺—is coordinated by the carboxylate function.^[12] The phosphonate coordination of the deprotonated ligand can be easily understood, since the double negative charge of the (non-esterified) phosphonate group of impa³⁻ gives this group a large electrostatic advantage over carboxylate for the coordination of a metal cation. Interpretation of the coordination switch to carboxylate upon double protonation is less straightforward. Transfer of one proton to [Pt(NH₃)₂(impa)]⁻ creates [Pt(NH₃)₂(impaH)]⁻, in which the carboxylate group is a considerably better base than the phosphonic acid monoanion (difference of 3 log units). In addition, the phosphonic acid monoanion is less sterically hindered than the phosphonate monoester of **1b**, so it is rather surprising that the carboxylate is coordinated and not protonated in [Pt(NH₃)₂(impaH₂)]⁺, whereas the opposite situation is found in **1b**. The coordination switch must therefore be due to steric strain favoring carboxylate coordination. We conclude that the five-membered ring of the [Pt(NH₃)₂(impaH₂)]⁺ system favors carboxylate over phosphonate coordination, whereas the opposite was seen above for the six-membered ring of the **1a/1b** system.

³¹P NMR chemical shift indicates the protonation status of phosphonate: ³¹P NMR chemical shifts of phosphorylated compounds depend on the electron density on phosphorus and on the bond angles, which affect *p*-orbital unbalancing and thus the shielding of the nucleus (see Ref. [26], p. 12). These two effects partly compensate in phosphates and phosphonates, so that protonation has relatively little effect on δ_p and is of opposite sign: protonation of the phosphate group causes a moderate upfield shift, whereas protonation of a phosphonate usually causes a moderate downfield shift.^[17] Inclusion of the phosphate or phosphonate group in a five-membered ring fixes the endocyclic O-P-O (phosphates) or O-P-C (phosphonates) bond angle to a small value, and causes a large downfield shift with respect to corresponding acyclic compounds, whereas inclusion in a six-membered ring has the opposite effect (see Ref. [26], p. 14). These known dependences were instrumental in the assignment of the various species occurring in the reaction between *cis*-[Pt(NH₃)₂(H₂O)₂]²⁺ and *N*-(phosphonomethyl)glycine (impaH₃).^[12] In this work we have observed a downfield shift of the phosphorus signal of **L**²⁻ upon protonation to **LH**₂ (from 9.3 to 13.4 ppm), as expected for protonation of phosphonate (vide supra). However, upon addition of only one equivalent of H⁺, generating the intermediate **LH**⁻, a slight *upfield* shift (to ≈ 9.1 ppm) was observed, suggesting that the phosphonate group is protonated only by the second equivalent; this observation provided support for carboxylate being the stronger base (thus being protonated by the first H⁺ equivalent).

More complex are the origins of the changes in δ_p upon coordination of **L**²⁻ and **LH**⁻ to *cis*-[Pt(NH₃)₂]²⁺. From Gorenstein's compilation of data (Ref. [26], p. 14), for instance, one expects that the fixation of the phosphonate group in

the six-membered P-O-Pt-S-C-C ring formed in **1b** should shift the phosphorus resonance upfield with respect to uncomplexed **LH⁻**. However, the inductive effect due to electron transfer from phosphonate to platinum should cause a downfield shift. The resulting moderate downfield shift observed between **LH⁻** ($\delta_p \approx 9.1$ ppm) and **1b** ($\delta_p \approx 11.0$ ppm) thus apparently corresponds to the sum of both effects, plus the effect of the conformational rearrangement.

Upon protonation of **1a** ($\delta_p \approx 6.4$ ppm) to **1aH⁺** ($\delta_p \approx 9.9$ ppm) in methanolic solution we observe a downfield shift, as expected for protonation of a phosphonate group.^[17]

Conclusion

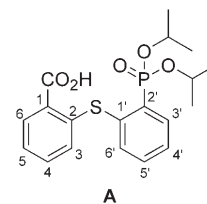
The newly synthesized ligand **L²⁻** proved to be a good chelator for platinum, reacting readily with *cis*-[Pt(NH₃)₂-(H₂O)₂]²⁺. The two anionic forms of acido groups in **L²⁻**—carboxylate and phosphonate—compete for platinum coordination. When one proton equivalent is added to the 1:1 complex, then both acido groups compete at the same time for Pt^{II} coordination and also for H⁺ binding. The carboxylate group, the stronger base (by about 1 log unit) in our system, turned out also to have a stronger intrinsic affinity for platinum. This conclusion could be inferred from the observation that in the crystal structure of the electroneutral complex [Pt**L**(NH₃)₂] (**1a**), the coordinating acido group is carboxylate, although the six-membered *S*-(*OC*) chelate ring is fairly strained. Upon addition of 1 proton equivalent, however, the combined effects of the stronger carboxylate basicity and steric strain accompanying carboxylate coordination induce a switch to phosphonate coordination, with concomitant protonation of carboxylate. In the rearranged, phosphonate-bound compound, [Pt(**LH**)(NH₃)₂]ClO₄ (**1b**), the six-membered *S*-(*OP*) chelate ring involving coordinated phosphonate seems practically strainless.

Experimental Section

General: The quality of the solvents used was RS. THF was purified with a PURESOLV apparatus developed by Innovative Technology Inc. Pyridine and DMF were freshly distilled and dried over calcium hydride under nitrogen pressure. Thioisalicic acid was purchased from Aldrich. ¹H, ¹³C, and ³¹P NMR spectra were recorded with Bruker DPX 250 MHz, and Bruker DRX 400 MHz spectrometers. ¹³C NMR spectra were recorded with decoupling of ¹H in broadband. The peak patterns are indicated as follows: s, singlet; d, doublet; t, triplet; sept, septuplet; m, multiplet. Spectra were recorded with TMS as internal standard, or with 85% phosphoric acid solution as external reference. ¹⁹⁵Pt NMR spectra were run with reference to an aqueous solution of Na₂PtCl₆. The coupling constants (*J*) are reported in Hertz (Hz). The mass spectra were recorded with a GC/MS Saturn 2000 with an ionic trap door and a Varian P-SIL 8CB Low BLEED/MS column, or on a Waters QTOF micro apparatus. Elemental analyses were obtained with a THERMOQUEST NA 2500 apparatus. The melting points were measured with a Kofler bench and are uncorrected. Thin layer chromatography (TLC) was performed on silica gel 60F₂₅₄ plates and results were viewed by UV. IR spectra were recorded either with a Perkin–Elmer 16 PC FT-IR instrument or with a Perkin–Elmer ATR universal FT-IR instrument.

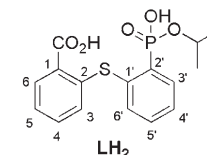
2-[2'-(Diisopropoxyphosphoryl)phenylsulfanyl]benzoic acid (**A**):

Diisopropyl 2-sulfanylphenylphosphonate^[13] (4.476 g, 16.3 mmol, 1.0 equiv) was diluted in freshly distilled pyridine (ca. 6 mL for 1 g of thiol) under nitrogen. 2-Iodobenzoic acid (4.047 g, 16.3 mmol, 1.0 equiv) and copper(I) oxide (1.167 g, 8.16 mmol, 0.5 equiv) were added and the reaction mixture was heated at 110 °C for four hours with vigorous stirring. The solution was cooled to 0 °C, acidified with HCl (37%), and stirred for one hour. The precipitated salts were filtered off, washed extensively with NaOH (10%), and discarded. The remaining alkaline filtrate was filtered once again, acidified to pH 1 with HCl (20%), and extracted with CH₂Cl₂. The organic layer was dried over magnesium sulfate and concentrated in vacuo to give an orange solid, which was further recrystallized from ethyl acetate and collected as a white solid (4.333 g, 11.0 mmol, 67%). M.p. 178 °C; ¹H NMR (250 MHz, CDCl₃): δ = 1.16 (d, ³J_{H,H} = 6.1 Hz, 6H; CH₃), 1.27 (d, ³J_{H,H} = 6.4 Hz, 6H; CH₃), 4.77 (dsept, ³J_{H,P} = 7.0, ³J_{H,H} = 6.1 Hz, 2H; CH), 6.74 (d, ³J_{H,H} = 7.9 Hz, 1H; H₆), 7.15 (dt, ³J_{H,H} = 7.6, ⁴J_{H,H} = 1.5 Hz, 1H; H₅), 7.24 (dt, ³J_{H,H} = 7.8, ⁴J_{H,H} = 1.3 Hz, 1H; H₄), 7.50 (ddt, ³J_{H,H} = 7.6, ⁴J_{H,P} = 3.3, ⁴J_{H,H} = 1.5 Hz, 1H; H₄), 7.56 (dt, ³J_{H,H} = 7.5, ⁴J_{H,H} = 1.4 Hz, 1H; H₅), 7.62 (dd, ³J_{H,H} = 7.5, ⁴J_{H,H} = 1.4 Hz, 1H; H₆), 7.99 (dd, ³J_{H,H} = 7.6, ⁴J_{H,H} = 1.5 Hz, 1H; H₃), 8.15 ppm (ddd, ³J_{H,P} = 14.2, ³J_{H,H} = 7.1, ⁴J_{H,H} = 1.7 Hz, 1H; H₃); ¹³C NMR (62.9 MHz, CDCl₃): δ = 23.7 (d, ³J_{C,P} = 5.0 Hz; CH₃), 23.9 (d, ³J_{C,P} = 3.8 Hz; CH₃), 71.7 (d, ²J_{C,P} = 6.3 Hz; CH), 124.6 (s; C₅), 127.7 (s; C₁), 128.62 (d, ²J_{C,P} = 14.5 Hz; C₃), 128.67 (s; C₆), 131.4 (s; C₃), 132.3 (s; C₄), 133.0 (s; C₅), 134.6 (d, ¹J_{C,P} = 196.2 Hz; C₂), 135.4 (d, ³J_{C,P} = 10.0 Hz; C₄), 136.8 (d, ³J_{C,P} = 7.5 Hz; C₆), 138.1 (d, ²J_{C,P} = 12.6 Hz; C₁), 142.6 (s; C₂), 170.0 ppm (s; CO₂H); ³¹P NMR (101 MHz, CDCl₃), δ = 14.6 ppm; IR (KBr): $\tilde{\nu}$ = 2980, 1694, 1464, 1203, 1001 cm⁻¹; MS: *m/z* (%): 395 [M+H]⁺ (24), 377 (12), 353 (48), 335 (44), 311 (43), 293 (100), 213 (8); elemental analysis (%), calcd for C₁₉H₂₃O₅PS: C 57.87, H 5.88, S 8.13; found: C 58.2, H 5.9, S 8.1.

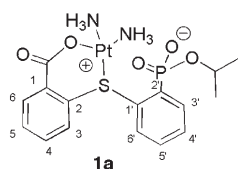


2-[2'-(Hydroxyisopropoxyphosphoryl)phenylsulfanyl]benzoic acid (**LH₂**):

The monohydrolysis step was carried out by mixing the phenylphosphonate **A** (993 mg, 2.5 mmol, 1 equiv) and sodium azide (1.309 g, 20.1 mmol, 8 equiv) in distilled water (ca. 100 mL for 1 g of phosphonate). The mixture was heated at 100 °C for three days. After cooling to room temperature, it was acidified with HCl (37%). Water was evaporated and the remaining residue was washed several times with CH₂Cl₂ (5 × 20 mL). The organic layer was dried over magnesium sulfate, filtered, and concentrated under reduced pressure. The crude phosphonic acid monoester **LH₂** (819 mg, 2.32 mmol, 92%) was recrystallized from ethyl acetate. M.p. 153 °C; ¹H NMR (250 MHz, CDCl₃): δ = 1.45 (d, ³J_{H,H} = 6.2 Hz, 6H; CH₃), 4.98 (dsept, ³J_{H,H} = 6.2, ³J_{H,P} = 9.2 Hz, 1H; CH), 6.53 (d, ³J_{H,H} = 8.0 Hz, 1H; H₆), 7.05 (dt, ³J_{H,H} = 7.5, ⁴J_{H,H} = 0.7 Hz, 1H; H₅), 7.25 (dt, ³J_{H,H} = 7.6, ⁴J_{H,H} = 1.5 Hz, 1H; H₄), 7.58 (m, 1H; H₄), 7.65 (m, 1H; H₅), 7.75 (m, 1H; H₆), 7.82 (dd, ³J_{H,H} = 7.8, ⁴J_{H,H} = 1.5 Hz, 1H; H₃), 8.09 (ddd, ³J_{H,P} = 13.1, ³J_{H,H} = 7.3, ⁴J_{H,H} = 1.7 Hz, 1H; H₃), 10.67 ppm (s, 2H; -OH); ¹³C NMR (62.9 MHz, CDCl₃): δ = 24.5 (d, ³J_{C,P} = 4.4 Hz; CH₃), 71.6 (d, ²J_{C,P} = 6.2 Hz; CH), 124.2 (s; C₅), 125.0 (s; C₁), 126.5 (s; C₆), 129.8 (d, ²J_{C,P} = 13.8 Hz; C₃), 132.5 (s; C₃), 133.3 (s; C₄), 133.6 (d, ⁴J_{C,P} = 3.1 Hz; C₅), 134.7 (d, ³J_{C,P} = 7.5 Hz; C₄), 134.8 (d, ³J_{C,P} = 9.4 Hz; C₆), 136.5 (d, ¹J_{C,P} = 200.6 Hz; C₂), 140.2 (d, ²J_{C,P} = 13.2 Hz; C₁), 144.7 (s; C₂), 171.8 ppm (s, CO₂H); ³¹P NMR (101 MHz, CDCl₃): δ = 17.8 ppm; IR (KBr): $\tilde{\nu}$ = 3381, 2981, 1654, 1467, 1155, 1009, 908 cm⁻¹; MS: *m/z* (%): 353 [M+H]⁺ (8), 335 (9), 311 (17), 293 (100), 213 (5); HRMS calcd for C₁₆H₁₇O₅NaPS: 375.0432; found: 375.0414; elemental analysis (%) calcd for C₁₆H₁₇O₅PS: C 54.54, H 4.86, S 9.10; found: C 54.9, H 4.9, S 9.1



cis-Diammine[2-[2'-(oxyisopropoxyphosphoryl)phenylsulfanyl]benzoato]-platinum(II) hydrate (1a**):** *cis*-Diamminedichloroplatinum (300 mg, 1 mmol, 1.0 equiv) and silver nitrate (334 mg, 1.99 mmol, 1.99 equiv) were dissolved in distilled water. The solution was stirred for 40 h at



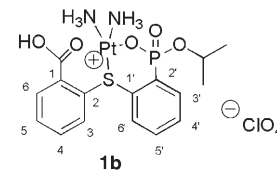
room temperature in the dark, and the silver chloride was removed by filtration, affording a colorless solution of *cis*-[Pt(NH₃)₂(H₂O)₂](NO₃)₂.

cis-[Pt(NH₃)₂(H₂O)₂](NO₃)₂ was slowly added to a stirred solution of **LH₂** (1 mmol) and potassium hydroxide

(2 mmol, 2 equiv) in water, and the mixture was stirred in the dark for one day at room temperature. After simple filtration, the benzoato platinum(II) complex **1a** was isolated as a white solid (498 mg, 0.86 mmol, 86%). To obtain monocrystals, **1a** (10 mg) was dissolved in MeOH (250 mL) and the solution was placed in an open Eppendorf tube, close to an open vessel filled with H₂O. Both vessels were covered hermetically. After 8 months, colorless monocrystals of **1a** suitable for X-ray diffractometry were collected. Decomp. 240 °C; solubility in methanol > 60 mg mL⁻¹; insoluble in water; ¹H NMR (400 MHz, DMF-d₇): δ = 1.30 (d, ³J_{H,H} = 6.2 Hz, 3H; CH₃), 1.46 (d, ³J_{H,H} = 6.1 Hz, 3H; CH₃), 4.68 (dsept, ³J_{H,P} = 8.0, ³J_{H,H} = 6.1 Hz, 1H; CH), 5.51 (s, 3H; NH₃), 5.83 (s, 3H; NH₃), 7.25 (dd, ³J_{H,H} = 7.7, ⁴J_{H,P} = 3.5 Hz, 1H; H₆), 7.45 (t, ³J_{H₄,H₅} = ³J_{H₄,H₃} = 7.5 Hz, 1H; H₄), 7.55 (dt, ³J_{H₅,H₄} = ³J_{H₅,H₆} = 7.5, ⁴J_{H₄,H₅} = 1.0 Hz, 1H; H₅), 7.70 (dt, ³J_{H,H} = 7.6, ⁴J_{H,H} = 1.4 Hz, 1H; H₄), 7.86 (dt, ³J_{H₅,H₄} = ³J_{H₅,H₆} = 7.5, ⁴J_{H,H} = 1.3 Hz, 1H; H₅), 8.00 (dd, ³J_{H,H} = 7.6, ⁴J_{H,H} = 1.0 Hz, 1H; H₃), 8.11 (ddd, ³J_{H,P} = 11.7, ³J_{H,H} = 7.5, ⁴J_{H,H} = 1.3 Hz, 1H; H₃), 8.46 ppm (dd, ³J_{H,H} = 7.9, ⁴J_{H,H} = 1.3 Hz, 1H; H₆); ¹³C NMR (162 MHz, CD₃OD): δ = 23.8 (d, ³J_{C,P} = 4.0 Hz; CH₃), 69.1 (d, ²J_{C,P} = 6.0 Hz; CH), 126.9 (s; C₃), 129.3 (d, ³J_{C,P} = 7.5 Hz; C₄), 129.9 (d, ³J_{C,P} = 11.1 Hz; C₆), 131.7 (s; C₁), 132.3 (s; C₅), 132.7 (s; C₆), 133.2 (d, ²J_{C,P} = 7.0 Hz; C₁), 134.1 (s; C₃), 134.3 (s; C₄), 134.5 (d, ²J_{C,P} = 6.6, C₅), 136.9 (d, ¹J_{C,P} = 170.0, C₂), 138.7 (s; C₂), 168.0 ppm (s, CO₂H); ³¹P NMR (162 MHz, DMF-d₇): δ = 3.5 ppm; ¹⁹⁵Pt NMR (53.7 MHz, DMF-d₇): δ = -2581 ppm; IR (neat): ν̄ = 3140, 1618, 1369, 1174, 987 cm⁻¹; MS: *m/z* (%): 580 [*M*+H]⁺ (100), 563 (53); HRMS calcd for C₁₆H₂₂O₅N₂O₃PtPS: 580.0635; found: 580.0617; elemental analysis (%) calcd for C₁₆H₂₁N₂O₅PPtS·1H₂O: C 32.16, H 3.88, N 4.69; found: C 31.4, H 4.0, N 4.6.

cis-Diammine[2-(2'-(hydroxyisopropoxyphosphorylato)phenylsulfanyl)-benzoic acid]platinum(II) perchlorate hydrate (**1b**): The benzoato platinum complex **1a** (56.0 mg,

0.097 mmol) was dissolved in methanol. Perchloric acid (20 μL, 0.097 mmol, 1.0 equiv) was added, the precipitated salt formed upon addition of 1,4-dioxane was collected, and a pure sample of the phosphonato platinum(II) complex **1b** was isolated by recrystallization from a methanol/dioxane (1:4) mixture as a white solid (35.3 mg, 0.053 mmol, 55%). Monocrystals were obtained through recrystallization from MeOH/THF. Decomp. 190 °C; Solubility in methanol, 6 mg mL⁻¹; virtually insoluble (< 1 mg mL⁻¹) in water; ¹H NMR (400 MHz, DMF-d₇): δ = 1.23 (d, ³J_{H,H} = 5.3 Hz, 3H; CH₃), 1.35 (d, ³J_{H,H} = 5.2 Hz, 3H; CH₃), 4.69 (sept, ³J_{H,H} = 6.3 Hz, 1H; CH), 5.11 (s, 1H; CO₂H), 5.19 (s, 3H; NH₃), 5.46 (s, 3H; NH₃), 7.16–7.22 (m, 1H; H₆), 7.45–7.59 (m, 2H; H₄, H₅), 7.66 (t, ³J_{H₄,H₃} = ³J_{H₄,H₅} = 7.2 Hz, 1H; H₄), 7.74–7.88 (m, 2H; H₅, H₃), 7.96 (dd, ³J_{H,H} = 6.4, ³J_{H,P} = 10.9 Hz, 1H; H₃), 8.36 ppm (d, ³J_{H,H} = 7.4 Hz, 1H; H₆); ³¹P NMR (162 MHz, DMF-d₇): δ = 7.1 ppm; ¹⁹⁵Pt NMR (53.7 MHz, DMF-d₇): δ = -2475 ppm; IR (neat): ν̄ = 1694, 1082, 1015, 891, 756 cm⁻¹; MS: *m/z* (%): 580 [*M*-ClO₄]⁺ (100), 563 (18); elemental analysis (%) calcd for C₁₆H₂₂ClN₂O₅PPtS·H₂O: C 27.53, H 3.47, N 4.01, S 4.59; found: C 27.2, H 3.5, N 3.9 S 4.5.



Isopropyl 2-(methylsulfanyl)phenylphosphonic acid

(3): Diisopropyl 2-(methylsulfanyl)phenylphosphonate^[13] (1.318 g, 4.57 mmol) and sodium azide (1.758 g, 8 equiv, 36.5 mmol) were dissolved in DMF and the system was heated to reflux for three days. The obtained solid was filtered, washed several times with acetone, and diluted in a small quantity of methanol. The product was acidified with Am-

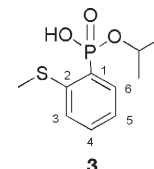


Table 2. Crystallographic data and structure refinement parameters for compounds **1a**, **1b**, and **LH₂**.

Compound	1a	1b	LH₂
empirical formula	[C ₁₆ H ₂₁ N ₂ O ₅ PPtS]·H ₂ O	[C ₁₆ H ₂₂ N ₂ O ₅ PPtS](ClO ₄)·H ₂ O	C ₁₆ H ₁₇ O ₅ PS
formula weight	597.48	697.94	352.33
crystal system	triclinic	monoclinic	monoclinic
space group	<i>P</i> 1 (no. 2)	<i>P</i> 2 ₁ / <i>c</i> (no. 14)	<i>P</i> 2 ₁ / <i>c</i> (no. 14)
unit cell dimensions			
<i>a</i> [Å]	9.529(6)	12.095(2)	9.498(5)
<i>b</i> [Å]	9.766(6)	14.046(2)	7.789(4)
<i>c</i> [Å]	12.299(7)	14.448(2)	24.201(12)
<i>α</i> [°]	106.91(2)		90
<i>β</i> [°]	101.71(2)	95.55(2)	100.470(10)
<i>γ</i> [°]	102.05(2)		90
<i>V</i> [Å ³]	1027.5(1)	2443.0(6)	1760.6(16)
<i>Z</i>	2	4	4
<i>ρ</i> _{calcd} [g cm ⁻³]	1.928	1.895	1.329
absorption coefficient [mm ⁻¹]	7.041	6.055	0.295
<i>θ</i> range [°]	2–23	2–24	2–22
Index ranges	-10 ≤ <i>h</i> ≤ 10 -10 ≤ <i>k</i> ≤ 10 -13 ≤ <i>l</i> ≤ 13	-13 ≤ <i>h</i> ≤ 13 -16 ≤ <i>k</i> ≤ 16 -16 ≤ <i>l</i> ≤ 16	-10 ≤ <i>h</i> ≤ 10 -8 ≤ <i>k</i> ≤ 8 -25 ≤ <i>l</i> ≤ 25
reflections collected	9154	16762	10600
independent reflections	2687	3856	2160
	[<i>R</i> _{int} = 0.0251]	[<i>R</i> _{int} = 0.0373]	[<i>R</i> _{int} = 0.1020]
data/restraints/parameters	2687/0/246	3856/30/291	2160/24/257
goodness-of-fit on <i>F</i> ²	1.096	0.934	1.023
observed reflections criterion	<i>I</i> > 2σ(<i>I</i>)	<i>I</i> > 2σ(<i>I</i>)	<i>I</i> > 2σ(<i>I</i>)
final <i>R</i> indices (observed data) ^[a]	<i>R</i> ₁ = 0.0149 <i>wR</i> ₂ = 0.0385	<i>R</i> ₁ = 0.0242 <i>wR</i> ₂ = 0.0625	<i>R</i> ₁ = 0.0635 <i>wR</i> ₂ = 0.1376
largest diff. peak [e Å ⁻³] and hole	0.542 and -0.326	0.896 and -0.426	0.336 and -0.206

[a] $R_1 = \sum ||F_o| - |F_c|| / \sum |F_o|$, $wR_2 = [\sum w(F_o^2 - F_c^2)^2 / \sum w F_o^2]^{1/2}$. Weighting: $w = 1 / [\sigma^2(F_o^2) + (aP)^2 + bP]$ where $P = (F_o^2 + 2F_c^2) / 3$.

berlyst 15 resin, and recrystallized from acetone to give a white solid (686 mg, 2.79 mmol, 61%). M.p. 112°C; ¹H NMR (250 MHz, CDCl₃): δ = 1.35 (d, ³J_{HH} = 6.2 Hz, 6H; CH₃); 2.47 (s, 3H; CH₃-S), 4.74 (dsept, ³J_{HH} = 6.2, ³J_{HP} = 1.5 Hz, 2H; CH), 7.15 (dt, ³J_{HH} = 7.4, ⁴J_{HP} = 3.4 Hz, 1H; H₃), 7.26–7.33 (m, 1H; H₃), 7.44 (t, ³J_{HH} = 7.4 Hz, 1H; H₄), 7.92 (dd, ³J_{HP} = 14.8, ³J_{HH} = 7.6 Hz, 1H; H₆), 11.31 ppm (s, 1H; OH); ¹³C NMR (62.9 MHz, CDCl₃): δ = 17.2 (s; CH₃-S), 24.3 (d, ³J_{CP} = 5.0 Hz; CH₃), 71.7 (d, ²J_{CP} = 6.3 Hz; CH), 124.7 (d, ³J_{CP} = 14.5 Hz; C₅), 127.2 (d, ³J_{CP} = 13.8 Hz; C₃), 128.5 (d, ¹J_{CP} = 196.9 Hz; C₁), 132.8 (d, ⁴J_{CP} = 2.5 Hz; C₄), 134.4 (d, ²J_{CP} = 9.4 Hz; C₆), 143.2 ppm (d, ²J_{CP} = 8.8 Hz; C₂); ³¹P NMR (101 MHz, CDCl₃): δ = 19.4 ppm; IR (KBr): $\tilde{\nu}$ = 1199, 1007, 910, 736 cm⁻¹; MS: *m/z* (%): 269 [M+Na]⁺ (100), 227 (70), 209 (40); HRMS calcd for C₁₀H₁₆O₃PS: 247.0558; found: 247.0555.

Crystallography

The data collections were performed at 293 K on a SMART-CCD Bruker diffractometer, by the ω -scan method, in the intervals $2 < \theta < 23^\circ$ (**1a**), $2 < \theta < 24^\circ$ (**1b**), and $2 < \theta < 22^\circ$ (**1H₂**). Empirical absorption corrections were applied by using the SADABS^[27] method in all cases. The structures were solved by direct methods (SIR97)^[28] and refined by full-matrix, least-squares on *F*² (SHELX-97^[29] and WINGX programs^[30]).

Compound **1H₂** shows a statistical enantiomeric disorder. Indeed, significant disorder was already apparent during the structure solution as the Fourier difference maps could only be interpreted in terms of two enantiomers occupying the same site. Careful selection of peaks from the electron-density maps allowed all non-hydrogen atom sites to be located. The atomic occupancies of each independent molecule were refined. The site occupancies for the enantiomeric pair were 68% and 32%, respectively. For compounds **1a** and **1b** anisotropic thermal parameters were assigned to all non-hydrogen atoms, whereas for **1H₂** only the atoms of the model showing the higher occupancy factors were refined anisotropically.

Hydrogen atoms were included in the refinement in calculated positions and refined using a riding model ($B(H) = 1.2 \times B(C_{\text{bonded}})(\text{\AA}^2)$), except for the hydrogens of the clathrated water molecule in (**1a**) which were located from a Fourier difference map.

Crystallographic data and analysis parameters are given in Table 2. All the diagrams were generated by using the ORTEP-III^[31] and Diamond^[32] programs.

CCDC-623705, CCDC-623706, and CCDC-623707 contain the supplementary crystallographic data for this paper. These data can be obtained free of charge from The Cambridge Crystallographic Data Centre via http://www.ccdc.cam.ac.uk/data_request/cif.

Acknowledgement

We are indebted to Dr. G. Bertho for NMR measurements, to Prof. F. Demartin for technical assistance with the X-ray acquisitions, and to Dr. S. Masson for helpful discussions. A generous gift of cisplatin from W. C. Heraeus GmbH is gratefully acknowledged. M.H. thanks the Ministère de la Recherche et des Nouvelles Technologies for a grant. Financial support from the Ministère des Affaires Étrangères and Egide (PAI Galilée 2005), which was essential for this collaborative project, is also gratefully acknowledged.

[1] P. J. O. O'Dwyer, J. P. Stevenson, S. W. Johnson in *Cisplatin: Chemistry and Biochemistry of a Leading Anticancer Drug* (Ed.: B. Lippert), Helvetica Chimica Acta, Zürich, **1999**, pp. 29–69.

- [2] Z. Guo, P. J. Sadler, *Angew. Chem.* **1999**, *111*, 1610–1630; *Angew. Chem. Int. Ed.* **1999**, *38*, 1512–1531.
- [3] G. Chu, *J. Biol. Chem.* **1994**, *269*, 787–790.
- [4] M. C. Christian, *Semin. Oncol.* **1992**, *19*, 720–733.
- [5] P. J. Bednarski, R. Gust, T. Spruss, N. Knebel, A. Ott, M. Farbel, R. Koop, E. Holler, E. von Angerer, H. Schonenberger, *Cancer Treat. Rev.* **1990**, *17*, 221–231.
- [6] A. Rosenfeld, J. Blum, D. Gibson, A. Ramu, *Inorg. Chim. Acta* **1992**, *201*, 219–221.
- [7] H. H. Lee, B. D. Palmer, B. C. Baguley, M. Chin, W. D. McFadyen, G. Wickham, D. Thorsbourne-Palmer, L. P. G. Wakelin, W. A. Denny, *J. Med. Chem.* **1992**, *35*, 2983–2987.
- [8] M. A. Jakupec, M. Galanski, S. Slaby, B. K. Keppler, *Eur. J. Cancer* **2002**, *38*, 29–30.
- [9] T. Klenner, P. Valenzuela-Paz, F. Amelung, H. Münch, H. Zahn, B. K. Keppler, H. Blum in *Metal Complexes in Cancer Chemotherapy* (Ed.: B. K. Keppler), VCH, Weinheim, **1993**, pp. 85–127.
- [10] K. Ajima, M. Yudasaka, T. Murakami, A. Maigné, K. Shiba, S. Iijima, *Mol. Pharm.* **2005**, *2*, 475–480.
- [11] C. Klumpp, K. Kostarelos, M. Prato, A. Bianco, *Biochim. Biophys. Acta* **2006**, *1758*, 404–412.
- [12] T. G. Appleton, J. R. Hall, I. J. McMahon, *Inorg. Chem.* **1986**, *25*, 726–734.
- [13] S. Masson, J.-F. Saint-Clair, A. Dore, M. Saquet, *Bull. Soc. Chim. Fr.* **1996**, *133*, 951–964.
- [14] S. Masson, J.-F. Saint-Clair, M. Saquet, *Synthesis* **1993**, 485–486.
- [15] R. Adams, A. Ferretti, *J. Am. Chem. Soc.* **1959**, *81*, 4927–4931.
- [16] A. Holy, *Synthesis* **1998**, 381–385.
- [17] M. Satre, J.-B. Martin, G. Klein, *Biochimie* **1989**, *71*, 941–948.
- [18] P. S. Pregosin, *Annu. Rep. NMR Spectrosc.* **1986**, *17*, 285–349.
- [19] A. G. Orpen, L. Brammer, F. H. Allen, O. Kennard, D. G. Watson, R. Taylor, *J. Chem. Soc. Dalton Trans.* **1989**, S1–S83.
- [20] P. Kapoor, V. Y. Kukushkin, K. Löqvist, A. Oskarsson, *J. Organomet. Chem.* **1996**, *517*, 71–79.
- [21] A. Hongo, S. Seki, K. Akiyama, T. Kudo, *Int. J. Biochem.* **1994**, *26*, 1009–1016.
- [22] M. J. Bloemink, J. P. Dorenbos, R. J. Heetebrij, B. K. Keppler, J. Reedijk, H. Zahn, *Inorg. Chem.* **1994**, *33*, 1127–1132.
- [23] M. Laforgia, L. Cerasino, N. Margiotta, M. A. M. Capozzi, C. Cardellicchio, F. Naso, G. Natile, *Eur. J. Inorg. Chem.* **2004**, 3445–3452.
- [24] J. M. Teuben, J. Reedijk in *Cisplatin: Chemistry and Biochemistry of a Leading Anticancer Drug* (Ed.: B. Lippert), Helvetica Chimica Acta, Zürich, **1999**, pp. 339–362.
- [25] D. Wauchope, *J. Agric. Food Chem.* **1976**, *24*, 717–721.
- [26] D. G. Gorenstein, *Phosphorus-31 NMR: Principles and Applications*, Academic Press, New York, **1984**.
- [27] G. M. Sheldrick, *SADABS*, University of Göttingen, **1996**.
- [28] A. Altomare, M. C. Burla, M. Camalli, G. Cascarano, C. Giacovazzo, A. Guagliardi, A. G. Moliterni, G. Polidori, R. Spagna, *J. Appl. Crystallogr.* **1999**, *32*, 115–119.
- [29] G. M. Sheldrick, SHELXL97, University of Göttingen, Germany, **1997**.
- [30] L. J. Farrugia, *J. Appl. Crystallogr.* **1999**, *32*, 837–838.
- [31] L. J. Farrugia, *J. Appl. Crystallogr.* **1997**, *30*, 565.
- [32] K. Brandenburg, DIAMOND, 3.0 ed., Crystal Impact GbR, Bonn, Germany, **1998**.

Received: November 3, 2006

Revised: February 5, 2007

Published online: April 17, 2007